Journal of ELECTRICAL ENGINEERING, VOL 72(2021), NO6, 381–387

sciendo

PAPERS

Influence of saturation levels on transformer equivalent circuit model

Yingying Wang, Xingyu Zhong, Xu Chen[1]

This paper presents a modelling approach for a transformer with different saturation levels. First, the magnetic field distributions at different saturation levels in the transformer are analyzed by using numerical simulations. Then, the characteristics of the leakage magnetic flux are analyzed, and the magnetic circuits with varying leakage reluctance topologies are modeled. Finally, based on the mature duality relationship between electric and magnetic circuits, the equivalent electric circuit models are obtained. These kinds of models embody the effect of different saturation levels on the connection points of the leakage flux branches, and it can fully reflect the various working states of the transformer. The accuracy of the models is verified by comparing the circuit simulation results with those of FEM transient simulations.

K e y w o r d s: duality principle, leakage flux, saturation level, transformer model

1 Introduction

The widely used single-phase transformer model is the STC (star circuit) model [1]. In the STC model, there is a star point, and each winding is connected through the star point. The leakage inductance is set between the port and the star point, and the excitation inductance branch is connected between the star point and the ground. The STC model can be easily extended to a single-phase multi-winding transformer model. The single-phase transformer model used in the EMTP software is the STC model. However, there is a deviation when the model is used to analyse the nonlinear problem of the transformer. Dick and Watson experimentally proved that placing the excitation branch at the star point in the STC model causes a large deviation, and suggested that the excitation branch should be connected to winding port closest to the core [2]. When the transformer has three or more windings, the leakage inductance value in the STC model is negative. Many scholars previously believed that the negative inductance in the STC model is the cause of the numerical oscillations during transient simulation [3]. However, recent studies by F.de León *et al* have shown that negative inductance is not the cause of oscillation [4]. For example, Simplorer or PSCAD will not oscillate when dealing with the circuits with negative inductance. The essential reason for the oscillation is the connection of the excitation branch. When the excitation branch is connected to the port close to the core winding, the STC model will not oscillate. However, the current research has not theoretically deduced the connection method of the excitation branch and the leakage inductance branch when the core is nonlinear.

When there are only two windings, the STC model is the well-known T model. The leakage inductance of the transformer in the T model is divided into two parts, and its equivalent circuit has only one excitation branch [5]. In the π model, there is only one leakage inductance, which is placed between the two excitation branches. The T model is suitable for most of the operating conditions of the transformer, however, as the transformer core is gradually saturated, the value of the leakage inductance on both sides of the T model changes [6]. Since the current flowing through the leakage inductance includes not only the excitation current but also the reflected current of the load, it is difficult to define a leakage inductance with the change of the excitation branch current in the circuit software. The leakage inductance in the T model can only be represented by a constant [7, 8]. Some scholars have studied the ratio of two leakage sensations and given some empirical results, but this method of correction cannot solve the problem fundamentally [9]. The T model cannot accurately represent the characteristics of the transformer under deep saturation. F. de León suggested that the π model has better accuracy than the T model in the case of deep saturation [10]. He demonstrated the advantages of the π model through experiments, and the difference between the inrush currents of the T and π models calculated can reach 73 %.

The placement of the magnetic flux leakage branch in the transformer equivalent circuit has a great impact on the accuracy of transient simulation. If the leakage flux is not properly connected, the simulated inrush current results of overvoltage problems will have a large error. Many scholars argue how to connect the leakage inductances reasonably in the circuit [11–13]. When transformer core operates at different saturation levels, the distributions of the leakage flux change. It means that the dumped magnetic circuit and the corresponding electrical circuit need

[1] School of Mechanical Electronic and Information Engineering, China University of Mining and Technology, Beijing, China, corresponding author: wangyy@cumtb.edu.cn.

https://doi.org/10.2478/jee-2021-0054, Print (till 2015) ISSN 1335-3632, On-line ISSN 1339-309X

Table 1. Typical points on the B–H Curve used in this paper

B (T)	0.1	0.6	1.5	1.65	1.75	1.8	1.84	1.88
H (A/m)	4.28	15.9	31.5	50.7	102	183	340	666
B (T)	1.9	1.93	1.95	1.98	2	2.06	2.28	3.28
H (A/m)	920	1567	2336	6300	1.05×10^4	2.2×10^4	2×10^5	1×10^6

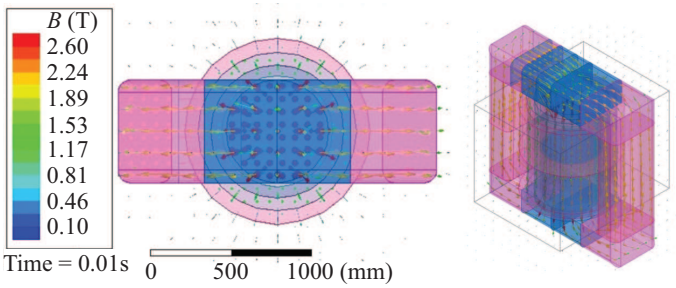

Fig. 1. A single-phase two-winding model and its magnetic field distribution

to change with the saturation levels. This paper studies the magnetic field distributions in the transformer at different saturation levels, and discusses the changes of leakage flux paths. Then, several typical magnetic circuits with various connections of leakage reluctance are obtained. The electrical circuit models are derived based on the mature duality principle between magnetic and electrical circuits [14]. The parameters of electrical circuits are determined by the nonlinear reluctance. Models at different saturation levels are verified by comparing the simulation results of the circuit models with FEM transient simulations.

2 Magnetic field distributions at different saturation levels

Magnetic field distributions at different saturation levels are analyzed by using the finite element method (FEM). A single-phase two-winding transformer is modeled by considering the nonlinearity of the magnetic core. Multiple sets of excitation voltages are applied to observe the magnetic field distribution at different saturation levels. Figure 1 shows the 16 MVA (110 kV/10.5 kV–50 Hz) transformer model with a high voltage winding as a primary coil and a low voltage winding as a secondary coil. The finite element numerical simulations in this paper were performed by using ANSYS.

The transformer is designed according to the rated voltage, and the designed peak value of the rated magnetic induction is at the place where the B–H curve changes from the linear zone to the transition zone (the B–H curve can be divided into linear zone, transition zone and saturation zone). When the excitation voltage is about 1.4 times the rated voltage, the magnetic induction intensity of the iron core changes rapidly in the transition zone; when the excitation voltage is about 1.6 times the rated voltage, the iron core is gradually saturated, and the magnetic field distribution inside the iron core increases significantly. So, the magnetic field distribution excited by 1.6 times the rated voltage is selected to show the distribution of magnetic flux leakage. Fig. 1 shows the magnetic field distribution when applying approximately 1.6 times the rated voltage at the primary winding terminal. The core of the transformer has a certain degree of saturation and the leakage flux in the air becomes obvious. This means that the leakage flux branch requires a more detailed analysis at different saturation levels to ensure that the transformer's lumped magnetic circuit model can accurately describe the transformer's magnetic field.

The grain-oriented electrical steel named B30P105 is used in this paper. The B–H curve used in this article is unique and does not change with the saturation level. The magnetization curve used in this article is the DC magnetization curve given by the iron core manufacturer. As the measured magnetizing curve usually cannot meet the requirements of saturation simulation [15, 16], it is usually expressed approximately by functions. In this paper, the magnetizing curves are extended by cubic functions (Akima interpolation method), and some typical DC magnetization data and the extended data are shown in Tab. 1.

In this part, we analyze the variation of the leakage flux distribution under different excitation states by observing the leakage flux on the cross section of the transformer, as shown in Fig. 2. In order to better observe the change of the leakage flux, only the magnetic flux in the core window is shown, and the magnetic flux inside the core is not shown. Figure 2(a) shows the flux distribution while the high voltage winding and the low voltage winding are excited by rated currents. Figure 2(b)–(d) show the simulation results when the excitation currents are gradually increasing. The value of flux density at the center point of the center column, noted by B_c, is used to

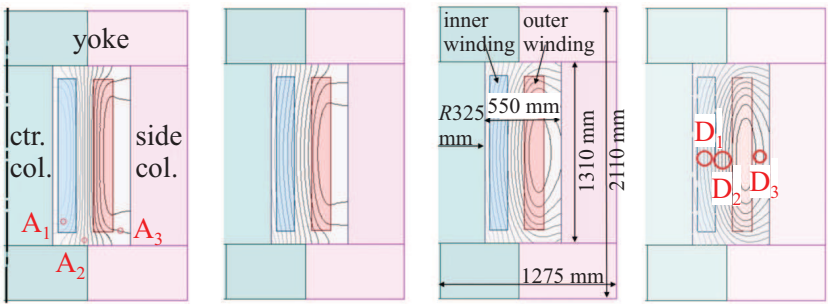

Fig. 2. Distribution of the leakage flux of the window at different saturation levels

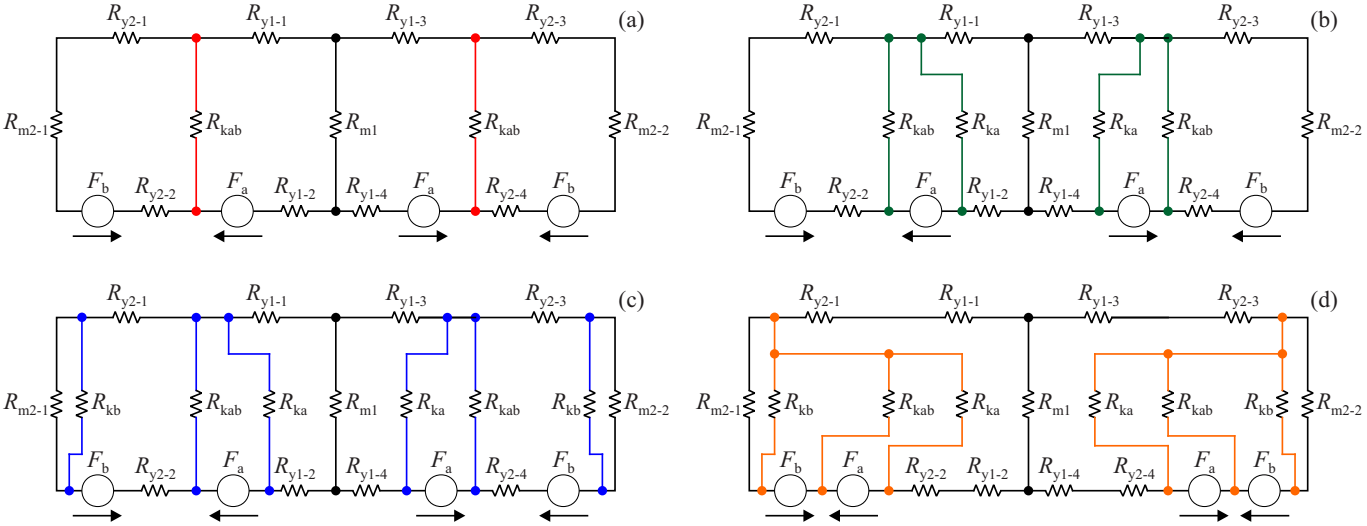

Fig. 3. Magnetic circuit models of four typical saturation levels

characterize the saturation of the core. In Fig. 2(a)–(d), the values of B_c are equal to 1.64 T, 2.02 T, 2.69 T, and 3.21 T, respectively. The values of the excitation voltage at each saturation level are 1 pu, 1.4 pu, 1.6 pu, and 2 pu, respectively.

As Fig. 2 shows, as the core is continuously saturated, the loop of the leakage flux changes. When the transformer operates at the rated state, the leakage flux between the two windings (A2) is linked with the inner and the outer winding, respectively. However, as the saturation level deepens, more and more leakage flux lines become to be linked with the outer high voltage winding. When the value of B_c is increased to 2.69 T and 3.2 T, the leakage flux between the two windings (D2) is almost entirely interlinked with the outer winding.

When the transformer operates at the rated state, the leakage flux (A1) is only linked with the inner winding, and it is not interlinked with the outer winding. However, when the core is deeply saturated, some of the leakage flux begins to be linked with the outer high voltage winding. Therefore, as the saturation deepens, this part of the flux no longer belongs to the leakage flux, but the main flux. Moreover, leakage flux between the high voltage winding and the side column (D3) cannot be ignored during deep saturation, as shown in Fig. 2(d).

As the saturation of the core is more severe, the leakage flux that links with the high voltage winding increases. For single-phase three-leg transformers of mature design, the parallel reluctance of the two side columns is usually smaller than that of the center column. Therefore, the center column is easier to saturate than the side columns, and the leakage flux tends to flow through the outer side column as the excitation current increases. Therefore, when the core is fully saturated, almost all the leakage flux is only interlinked with the outer winding.

3 Magnetic and electric circuits at different saturation levels

The paths of the leakage flux change at different saturation levels. These changes not only affect the value of the leakage parameters, but also affect their connection points in the topology. Therefore, when modelling transformers which may work at various saturation levels, it is recommended to consider the changes of leakage parameters.

Magnetic circuit models for four typical saturation levels are established as shown in Fig. 3(a)–(d). Here F_a and

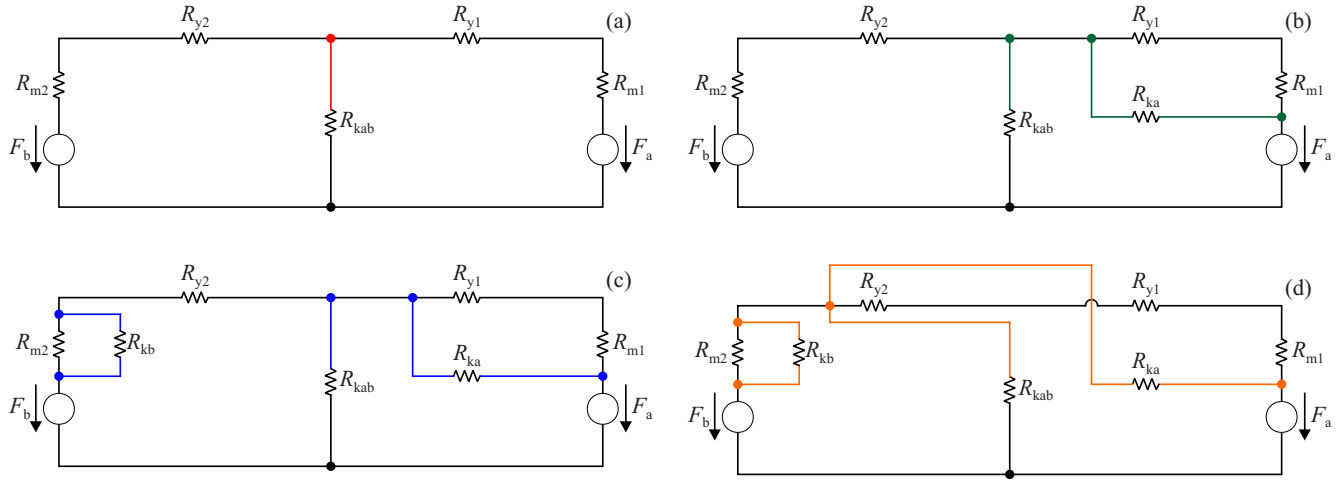

Fig. 4. Simplified magnetic circuit models based on symmetry

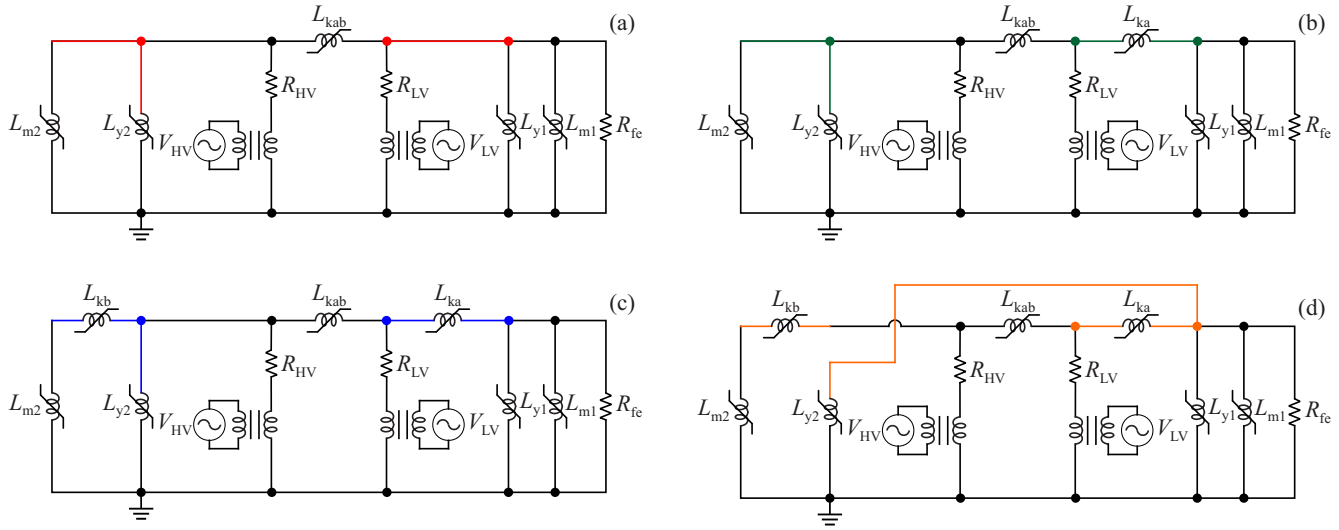

Fig. 5. Equivalent circuit models at different saturation levels: (a) – S1, (b) – S2, (c) – S3, and (d) – S4

F_b represent the magnetomotive forces of the low voltage winding and the high voltage winding, respectively. R_{mi} represents the reluctance of the iron cores, R_{yi} represent the reluctance of the yokes. R_{kab} represents the reluctance between the low voltage winding and the high voltage winding. R_{ka} represents the reluctance between the low voltage winding and the center column. R_{kb} represents the reluctance between the high voltage winding and the side column. When the transformer core has a low flux density, only R_{kab} is considered, and it is connected between the two segments of the yoke. As the core is gradually saturated, R_{ka} and R_{kb} need to be considered as shown in Fig. 3(b) and 3(c). When the core is deeply saturated, the connection points of R_{ka} and R_{kb} in the magnetic circuit will change, as shown in Fig. 3(d).

The focus of drawing a magnetic circuit diagram is the placement of magnetomotive force F_a and F_b in the magnetic circuit. The principle of placement is to ensure that the magnetic circuit with F_a and F_b is equivalent to the magnetic flux circuit in the magnetic field. According to this principle, the magnetic circuit topology shown in Fig. 3 can be drawn. Assuming that the internal magnetic field of the single-phase three-leg transformer is symmetrically distributed in the left and right, up and down directions, the magnetic scalar potential of the symmetric node in the magnetic circuit is the same. Taking the central column as a reference, connect the same points with the same magnetic scalar potential, and then the magnetic circuit can be simplified as shown in Fig. 4. After simplification, the value of magnetic resistance in the magnetic circuit is also calculated according to the connection relationship of series or parallel.

Then, according to the dual principle between the magnetic and electric circuits, the circuit models, noted by S1, S2, S3, S4, can be obtained as shown in Fig. 5. The dual principle is a method of converting the flux equation of the magnetic circuit topology into a node voltage equation, and then the circuit topology can be conveniently obtained. The change of the closed path of the leakage magnetic flux affects the connection point of the leakage

magnetic resistance in the magnetic circuit. As a result, the loop flux equations corresponding to the magnetic circuit will change. Therefore, the node voltage equation obtained by the conversion of the magnetic circuit equation changes, which is reflected in the change of the connection node of the magnetic leakage branch in the circuit topology.

In Fig. 5, R_{HV} and R_{LV} represent the resistance of the primary and secondary windings. The core loss corresponding to each reluctance can be represented by a variable resistance, whose value may change with the saturation degree. In the final circuit topology, the resistance that characterizes the core loss can be respectively connected with each part of the core in parallel. Since the core loss problem is not the focus of the analysis in this paper, it is represented by a single resistance R_{fe} and connected in parallel with R_{m1}. The number of leakage inductances and the junction point of the leakage flux branch change with the saturation level.

4 Verification of circuit models

The equivalent circuit simulation results are compared with the FEM analysis to verify the validity of the models in Fig. 5. Before implementing circuit simulations, the circuit parameters need to be determined. Usually, the transformer port test results are used to determine the equivalent circuit model parameters. This method can determine the parameters of the simple circuit model under the rated state. As the transformer manufacturer does not perform the saturation test, the equivalent circuit parameters in the saturated state cannot be obtained from the test parameters. Even if an overvoltage test is performed, there are theoretical difficulties in using the voltage and current waveforms measured by the port to determine the circuit parameters due to nonlinear problems, and the use of limited port characteristics is not sufficient to determine so many parameters in a complex circuit topology.

Methodology in [17] is considered for estimating circuit parameters, which is performed based on the magnetic field distribution under different excitations. The nonlinear inductance is derived by the nonlinear reluctance, which is determined by the flux pass though and the magnetic energy in them. The energy regions and the flux integral sections for reluctance are shown in Fig. 1. The nonlinear reluctance in the magnetic circuit is calculated by

$$R = \frac{2W}{\phi^2} = \frac{\iiint_V \boldsymbol{H} \cdot \boldsymbol{B} \mathrm{d}V}{\left(\iint_S \boldsymbol{B} \cdot \mathrm{d}\boldsymbol{S}\right)^2}, \tag{1}$$

where R represents reluctance, W represents the energy of the magnetic field, ϕ represents magnetic flux, $\boldsymbol{H}$ represents magnetic field strength, $\boldsymbol{B}$ represents the magnetic flux density. Reference [17] proposed a parameter determination method for complex equivalent circuit, but it does not analyze the variation of the circuit topologies under different saturation levels, and the equivalent circuit topology it used is not the most reasonable.

Closing simulations are performed to check the performance of the transformer models at different saturation levels. A sinusoidal voltage source with a frequency of 50 Hz is placed on the high voltage side of the equivalent circuit model, and the secondary low voltage side remains open. No-load closing processes of the transformer equivalent circuits under different saturation levels are simulated, and the saturation levels can be changed by adjusting the closing phase angle. At the initial moment of the closing process, excitation with different closing angles will cause the transformer to enter different saturation states. If the excitation voltage is set to $u = U_m(sin\omega t + \phi_0)$, when the closing angle ϕ_0 is equal to $90°$, the transformer will directly enter the steady state (without considering the remanence), and there will be no overvoltage; when ϕ_0 is equal to $0°$, the transformer will withstand twice the rated voltage at the moment of closing.

We check the inrush current of several equivalent circuit models at the closing angles of $30°$, $70°$, and $80°$, and compare inrush current results with the FEM simulation results. Then, the accuracies of several topologies can be analyzed by comparing the peak currents of different saturation levels with the FEM simulation results. According to the results, as the degree of saturation deepens, the error of the topology at rated time becomes larger and larger, and it is very important to select a suitable topology to obtain accurate results.

Figure 6 shows the inrush currents of the four topologies (S1, S2, S3, S4) under different saturation levels while the closing phase angles are $80°$, $70°$, and $30°$, respectively. As Fig. 6(a) shows, when the closing phase angle is $80°$, that is, when the iron core is slightly saturated, the peak currents of several circuit topologies are approximately the same and are consistent with the FEM simulation results. As the saturation level deepens, the difference in peak currents increases. In the state shown in Fig. 6(b), the current obtained by FEM simulation is similar to topology S2 and S3. In the state shown in Fig. 6(c), the peak currents are significantly different due to deep saturation of the core, and compared with the FEM results, the errors of the four topologies are 60 %, 51 %, 45 %, and 1.2 %, respectively.

We compare the inrush currents of different topologies with that simulated by commercial power system simulation software. In the software, the ϕ–i curve of the single-phase transformer model is fitted according to the rated parameters. Since the core loss is not considered in the FEM simulation, the core loss is also ignored when setting the transformer in the commercial software. According to the simulation results shown in Fig. 6(c), the commercial software has a large error when analysing deep saturation problem.

Therefore, the influence of the magnetic circuit topology on the calculation of the inrush current is more obvious as the saturation level deepens. When building a

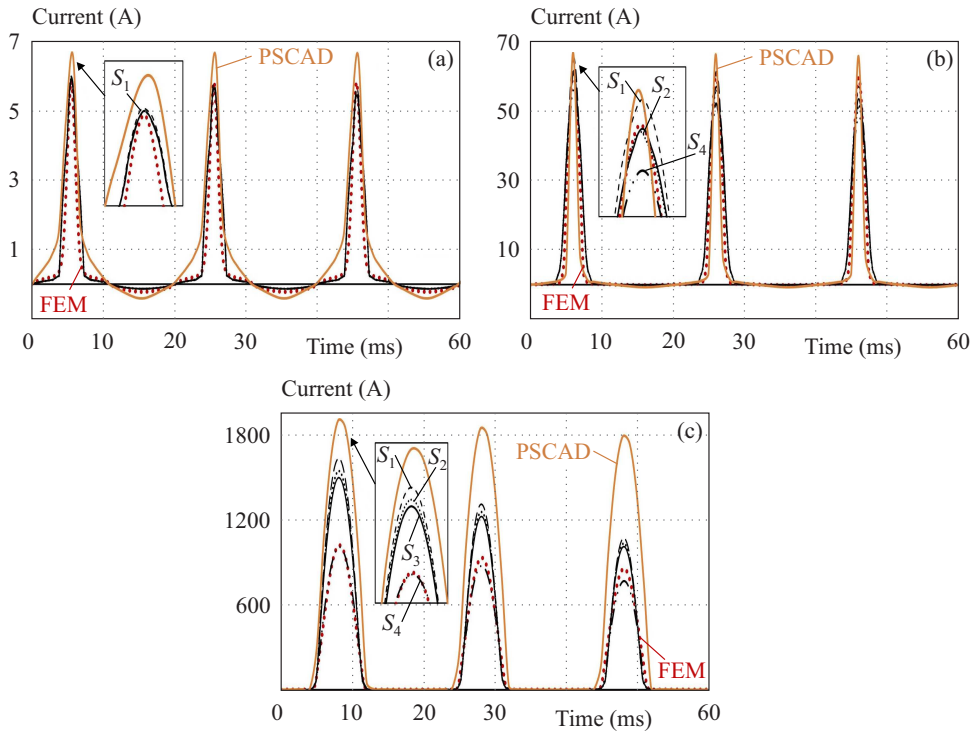

Fig. 6. Inrush currents obtained by circuit simulations, FEM analysis, and commercial circuit simulation software when the closing phase angles are: (a) – 80 °, (b) – 70 °, (c) – 30 °

transformer model, it is recommended to select the appropriate model based on the estimated operating state of the transformer.

5 Conclusions

In this paper, the influence of core saturation on the closed path of the leakage magnetic field is analyzed. As the saturation of the core deepens, more and more leakage flux flow through the side columns to close, and these leakage fluxes are linked to the high voltage windings. This is because the center column is more saturated than the side column, and it also reflects the influence of the transformer structure size on the magnetic field distribution and the magnetic circuit topology. By considering the changes of the connection points of leakage flux branches, several typical magnetic circuits and circuit topologies at different saturation levels are given.

Closing process at different saturation levels are simulated, and as the saturation level deepens, the differences between simulated currents obtained based on different topologies increase significantly. Taking the simulation with 30 °closing angle as an example, the difference between the peak currents obtained by the topology S1 and the finite element calculation is up to 60 %, and that obtained by the topology S4 is 1.2 %. When implementing transient problem simulation, it is recommended to estimate the level of overvoltage and select a topology that is as simple as possible but meets the accuracy requirements.

References

[1] F. Blume, A. Boyajian, G. Camilli, *et al*, *Transformer engineering*, 2 nd ed. New York, Wiley, 1951.

[2] E. P. Dick and W. Watson, "Transformer Models for Transient Studies Based on Field Measurement", *IEEE Transactions on Power Apparatus & Systems*, vol. 100, no. 1, pp. 401- 409, 1981.

[3] X. Chen, "Negative Inductance and Numerical Instability of the Saturable Transformer Component in EMTP", *IEEE Transactions on Power Delivery*, vol. 15, no. 4, pp. 1199- 1204, 2000.

[4] S. Jazebi, S. E. Zirka, M. Lambert *et al*, "Duality Derived Transformer Models for Low-frequency Electromagnetic Transients Part I" Topological Models", *IEEE Transactions on Power Delivery,*, vol. 31, no. 5, pp. 2410–2419, 2016.

[5] A. Martinez and B. A. Mork, "Transformer Modeling for Low-and Mid-frequency Transients-A review", *IEEE Transactions on Power Delivery*, vol. 20, no. 2, pp. 1525–1632, 2005.

[6] Boyajian, "Resolution of Transformer Reactance: Into Primary and Secondary Reactances", *AIEE Transactions*, vol. 44, no. 8, pp. 842–846, 1925.

[7] X. Deng, E. Cheng, and W. Wang, "A Novel Transformer with Adjustable Leakage Inductance", *International Journal of Applied Electromagnetics and Mechanics*, vol. 55, no. 1, pp. 29–43, 2017.

[8] C. Park, H. Lee and B. Lee, "A Study on the Design Parameters of Inductive Power Transformers", *International Journal of Applied Electromagnetics and Mechanics*, vol. 39, no. 1, pp. 809–815, 2012.

[9] A. Martinez-Velasco, R. Walling, B. A. Mork *et al*, "Parameter Determination for Modeling System Transients-part III: Transformers", *IEEE Transactions on Power Delivery*, vol. 20, no. 3, pp. 2051–2062, 2005.

[10] F. de León, A. Farazmand, and P.Joseph, "Comparing the T and π Equivalent Circuits for the Calculation of Transformer Inrush Currents", *IEEE Transactions on Power Delivery*, vol. 27, no. 4, pp. 2390–2397, 2012.

[11] E. Zirka, Y. I. Moroz, C. M. Arturi *et al*, "Topology-correct Reversible Transformer Model", *IEEE Transactions on Power Delivery*, vol. 27, no. 4, pp. 2037–2045, 2012.

[12] A. Mork, F. de León, and D. Ishchenko, "Hybrid Transformer Model for Transient Simulation-Part I" Development and Parameters", *IEEE Transactions on Power Delivery*, vol. 22, no. 1, pp. 248–255, 2007.

[13] S. Jazebi, J. A. Martinez, and F. de León, "Duality-derived Transformer Models for Low-frequency Electromagnetic Transients – Part II: Complementary Modeling Guidelines", *IEEE Transactions on Power Delivery*, vol. 31, no. 5, pp. 2420–2429, 2016.

[14] R. Slemon, "Equivalent Circuits for Transformers and Machines Including Nonlinear Effects", *Proceedings of the IEE – Part IV: Institution Monographs*, vol. 100, no. 5, pp. 129–143, 1953.

[15] D. Miyagi, T. Yamazaki, D. Otome *et al*, "Development of Measurement System of Magnetic Properties at High Flux Density Using Novel Single-sheet Tester", *IEEE Transactions on Magnetics*, vol. 45, no. 10, pp. 3889–3892, 2009.

[16] Y. Li, X. Geng, and C. Zhang, "Improved 3-D Magnetic Properties Measurement of Silicon Steel Laminations Based on a Novel Sensing Structure", *IEEE Transactions on Magnetics*, vol. 53, no. 11, pp. 6101404, 2017.

[17] Y. Wang and J. Yuan, "Calculation Approach of Reluctance in the Magnetic Circuit of Transformer Employed to Convert into Equivalent Electric Circuit," *COMPEL*, vol. 37, no. 6, pp. 1668–1677, 2018.

Received 22 July 2021

Yingying Wang received her PhD degree from Tsinghua University, Beijing, China, in 2018. She is currently an assistant researcher with School of Mechanical Electronic and Information Engineering, China University of Mining and Technology. Her current research interests include the EMC in power systems and computational electromagnetics.

Xingyu Zhong received his Bachelor's degree in electrical engineering from China University of Mining and Technology, Beijing, China. He is currently a graduate student at China University of Mining and Technology. His research fields are electromagnetic field calculation methods, nonlinear modeling of magnetic materials.

Xu Chen received his Bachelor's degree in electrical engineering from China University of Mining and Technology. He is currently a graduate student at China University of Mining and Technology. His research field is multiphysics analysis of high-voltage electrical devices.